Thermochimica Acta, 196 (1992) 495–502
Elsevier Science Publishers B.V., Amsterdam

A new master plot using the differential method in kinetic analysis of non-isothermal TG data

E.H. Kim [a], J.J. Park [a], J.H. Park [a,1], I.S. Chang [a] and C.S. Choi [b]

[a] *Nuclear Chemical Engineering Research Division, Korea Atomic Energy Research Institute, P.O. Box 7, Daeduk-Danji, Dae-Jeon 302-343 (Korea)*
[b] *Department of Chemical Engineering, Sogang University, Seoul 121-742 (Korea)*

(Received 17 April 1991)

Abstract

A new master plot developed from the differential method is proposed, which can give information about the reaction mechanism and the activation energy simultaneously from non-isothermal TG data. The applicability of the master plot is confirmed by comparing the results of kinetic analysis with those published for the thermal decomposition of $CaCO_3$ in an air atmosphere. The results are in good agreement with those previously published.

INTRODUCTION

Kinetic analysis in the solid state using non-isothermal TG can be classified into two categories, namely differential [1–3] and integral methods [4,5]. In these methods, several attempts have been made to determine the mechanism and kinetic parameters of a solid process by graphical analyses, which are often called "master plots". The concept of master plots for analyzing kinetic data from non-isothermal TG was introduced by Ozawa [6]. Satava and Skvara [7] proposed the use of master curves to determine mechanism and kinetic parameters by the integral method suggested by Doyle [4] and Zsako [5]. Reich and Stivala [8] also suggested a master curve obtained by integral methods from the ratio of $g(\alpha)$ and heating rate determined from two TG curves obtained at different heating rates. Recently, Criado [9] and Criado et al. [10] proposed various types of master curves involving the combination of differential and integral methods.

In spite of these studies, information for reaction kinetics such as reaction mechanism and activation energy could not be determined simultaneously. Also, master curves originating from differential methods have not yet appeared in the published literature. In this paper, a new graphical

---

[1] Author to whom correspondence should be addressed

method developed from the differential approach [1–3] is proposed, which can give information about reaction mechanism and activation energy simultaneously from non-isothermal TG data. The validity of the method is confirmed by comparing the kinetic analysis results for the thermal decomposition reaction of $CaCO_3$ in an air atmosphere with the published ones [9,11].

THEORY

The reaction rate of a solid state process can be described by the well-known general kinetic law

$$\frac{d\alpha}{dt} = kf(\alpha) \tag{1}$$

where α is the degree of conversion, k is the reaction rate constant and $f(\alpha)$ is a function depending on the decomposition mechanism. The rate constant (k) depends on the absolute temperature (T) according to the Arrhenius equation

$$k = A\,\exp(-E/RT) \tag{2}$$

where A, E and R are the pre-exponential factor, activation energy and gas constant, respectively.

From eqns. (1) and (2), we obtain

$$\frac{d\alpha}{dt} = A\,\exp(-E/RT)f(\alpha) \tag{3}$$

and, if we take natural logarithms, we obtain for a particular degree of conversion α_i

$$\ln\left(\frac{d\alpha}{dt}\right)_i = \ln[Af(\alpha_i)] - \left(\frac{E}{R}\right)\left(\frac{1}{T_i}\right) \tag{4}$$

where $(d\alpha/dt)_i$ and T_i are the reaction rate and temperature at which α_i was reached. For a particular degree of conversion α_i, the values of $(d\alpha/dt)_i$ and T_i can be determined from the non-isothermal TG data and the differential thermogravimetric (DTG) curves obtained at various heating rates. The plot of $\ln(d\alpha/dt)_i$ vs. $1/T_i$ gives a straight line, as shown in Fig. 1. The value of E can be directly determined from the slope, while the intercept of the line gives the value of $\ln A = \ln f(\alpha)$. Function $f(\alpha)$ is in most cases of the form [12]

$$f(\alpha) = (1-\alpha)^n \alpha^m [-\ln(1-\alpha)]^p \tag{5}$$

where m, n and p are constants. Functions $f(\alpha)$ for each mechanism are shown in Table 1. If the activation energy scarcely varies with the progress of reaction, the difference in the values of intercepts of a particular

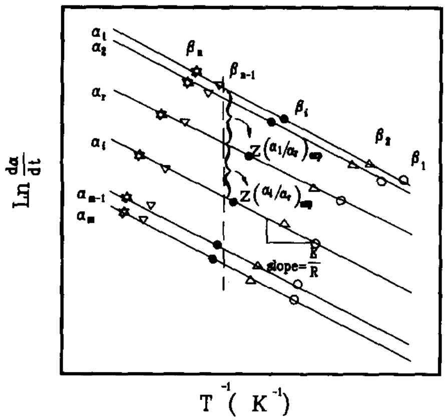

Fig. 1. Graphs for obtaining activation energy and $z(\alpha_i/\alpha_r)_{\text{exp}}$ value.

iso-conversion line and a reference one (subscripted r) can be obtained from eqn. (4) as

$$\ln\left(\frac{d\alpha}{dt}\right)_i - \ln\left(\frac{d\alpha}{dt}\right)_r = \ln f(\alpha_i) - \ln f(\alpha_r) \tag{6}$$

Because the values of $\ln(d\alpha/dt)_i - \ln(d\alpha/dt)_r$ can be obtained from experiments and those of $\ln f(\alpha_i) - \ln f(\alpha_r)$ can be determined theoretically, eqn. (6) can be simply re-written as eqn. (7)

$$z(\alpha_i/\alpha_r)_{\text{exp}} = z(\alpha_i/\alpha_r)_{\text{th}} \tag{7}$$

TABLE 1

Commonly used mathematical expressions of $f(\alpha)$ for solid state reactions

$f(\alpha)$	Symbol	Reaction mechanism
α^{-1}	D_1	One-dimensional diffusion
$[-\ln(1-\alpha)]^{-1}$	D_2	Two-dimensional diffusion
$[(1-\alpha)^{-1/3}-1]^{-1}(1-\alpha)^{1/3}$	D_3	Three-dimensional diffusion
$(1-\alpha)^{1/2}$	R_2	Two-dimensional phase boundary
$(1-\alpha)^{1/3}$	R_3	Three-dimensional phase boundary
$(1-\alpha)$	A_1	First order reaction
$(1-\alpha)[-\ln(1-\alpha)]^{1/2}$	A_2	Two-dimensional nucleation and growth
$(1-\alpha)[-\ln(1-\alpha)]^{1/3}$	A_3	Three-dimensional nucleation and growth
$(1-\alpha)^{1/5}$	$N_{1/5}$	One-fifth order
$(1-\alpha)^{1/3}$	$N_{1/3}$	One-third order
$(1-\alpha)^{1/2}$	$N_{1/2}$	One-half order
$(1-\alpha)^{2/3}$	$N_{2/3}$	Two-thirds order
$(1-\alpha)$	N_1	First order
$(1-\alpha)^{1/5}$	$N_{1/5}$	One and one-half order
$(1-\alpha)^2$	N_2	Second order

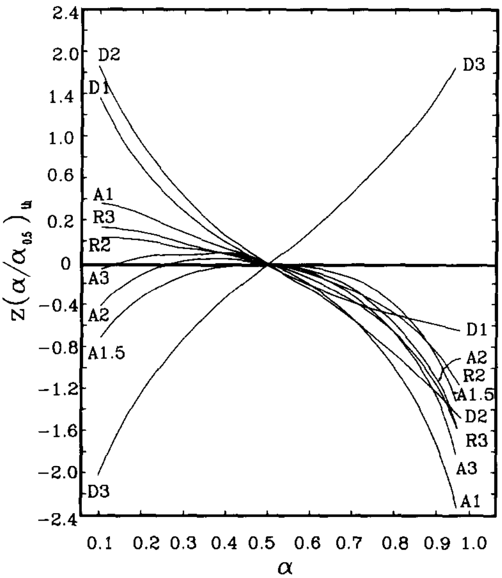

Fig. 2. The master curves $z(\alpha_i/\alpha_{0.5})_{th}$ of different solid state reaction mechanisms.

As can be seen in Fig. 1, $z(\alpha_i/\alpha_r)_{exp}$ is the difference in the values of intercepts of a particular iso-conversion line and a reference one, it can vary according to α_i and it depends on the reaction mechanism, regardless of heating rate. The values of $z(\alpha_i/\alpha_r)_{th}$ can be simply determined for the

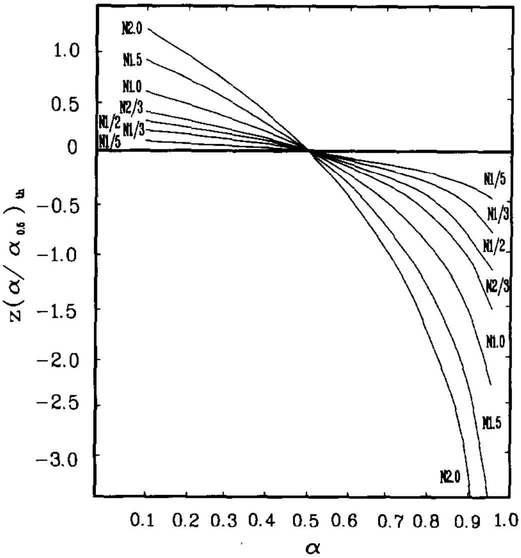

Fig. 3. The master curves $z(\alpha_i/\alpha_{0.5})_{th}$ of different reaction order mechanisms.

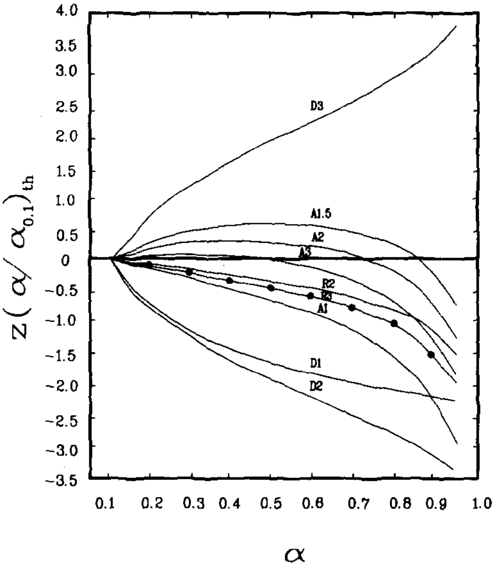

Fig. 4. The master curves $z(\alpha_i/\alpha_{0.1})_{\text{th}}$ of different solid state reaction mechanisms and $z(\alpha_i/\alpha_r)_{\text{exp}}$ of the thermal decomposition reaction of $CaCO_3$ in an air atmosphere.

different reaction mechanisms shown in Table 1, and the plot of $z(\alpha_i/\alpha_r)_{\text{th}}$ vs. α can be used as a master plot, which is a useful tool for the determination of kinetic mechanisms with comparison of $z(\alpha_i/\alpha_r)_{\text{exp}}$. Various master plots can be also obtained by taking a different reference

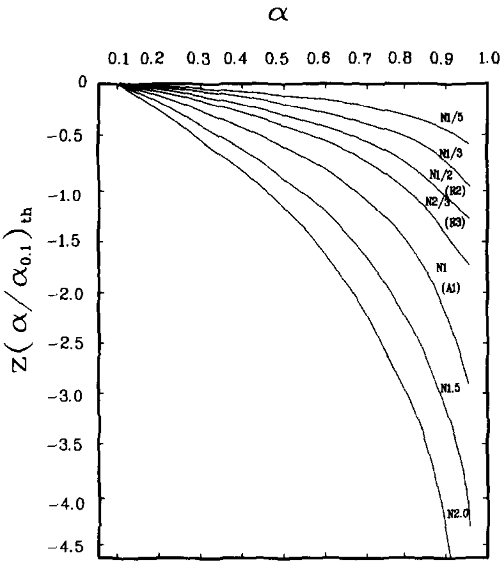

Fig. 5. The master curves $z(\alpha_i/\alpha_{0.1})_{\text{th}}$ of different reaction order mechanisms.

iso-conversion line. When $\alpha_r = 0.5$, typical master curves based on the various solid state reaction mechanisms and reaction order mechanisms are shown in Figs. 2 and 3; those when $\alpha_r = 0.1$ are shown in Figs. 4 and 5, respectively.

EXPERIMENTAL

Commercial grade limestone from the Gaduk mine in Korea was used for the experiment. This carbonate exhibits the following chemical composition: SiO_2, 1.2%; Fe_2O_3, 0.1%; Al_2O_3, 0.1%; MgO, 0.8%; CaO, 54.2%; loss on ignition, 43.3%. Thermogravimetric experiments were carried out in a thermal balance (Setaram TG–DTA 92) with heating rates of 2, 3.5, 5, 7 and 10 K min^{-1} in an air atmosphere (flow rate 50 cm^3 min^{-1}). The sample weight was about 10 mg for all the experiments, and the sample holder used was a cylindrical alumina cup about 6.0 mm in diameter and 5.0 mm in depth.

RESULTS AND DISCUSSION

As can be seen in Fig. 2, master curves $z(\alpha_i/\alpha_{0.5})_{\mathrm{th}}$ for different solid state mechanisms are well separated in the low conversion region, but it is not easy to distinguish the various mechanisms in the high conversion region. The shape of this master plot is similar to that of the previously proposed one [9]. Since the purpose of using a master plot is to ascertain a reaction mechanism simply and precisely from reaction rate data, master curves for different reaction mechanisms should be well separated from each other. In this study, various master plots could be obtained with variation of α_r and master plots for $\alpha_r = 0.1$ and 0.9 were found to have good separability for practical purpose. Since they are symmetrical one with the other, the master plot for $\alpha_r = 0.1$ is shown representatively in Fig. 4. As can be seen in Fig. 4, master curves for different solid state reaction mechanisms are well separated over the full range of degree of conversion. In the case of reaction order mechanisms, as can be seen in Figs. 3 and 5, the master curves for both $z(\alpha_i/\alpha_{0.5})_{\mathrm{th}}$ and $z(\alpha_i/\alpha_{0.1})_{\mathrm{th}}$ are well separated. Thus, since the master plots shown in Figs. 3, 4 and 5 are well separated over the full range of degree of conversion, these can be used in discerning the reaction mechanisms easily from reaction rate data.

In order to confirm the correctness of this master plot, it has been applied to the thermal decomposition reaction of $CaCO_3$. The thermogravimetric and differential thermogravimetric curves of $CaCO_3$ decomposition are plotted vs. heating rate in Fig. 6. From these data, the plots of $\ln(\mathrm{d}\alpha/\mathrm{d}t)_i$ vs. $1/T_i$ for different degrees of conversion could be obtained, and give straight lines as shown in Fig. 7. The values of E determined from their slopes are almost constant, as shown in Table 2. The mean value is

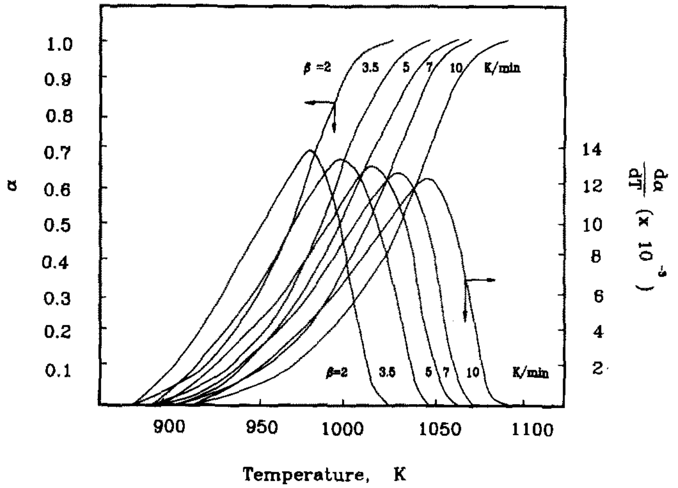

Fig. 6. TG and DTG curves for the thermal decomposition reaction of $CaCO_3$ in an air atmosphere at different heating rates.

49.67 ± 1.95 kcal mol^{-1}, which is in good agreement with the published value of 46.19 kcal mol^{-1} [11]. Experimental results $[z(\alpha_i/\alpha_{0.1})_{exp}]$ are plotted in Fig. 4. As can be seen, the thermal decomposition reaction of $CaCO_3$ follows the reaction mechanism of a three-dimensional phase boundary, which is the same as the previously published findings [10,11]. Consequently, the proposed master plot can be precisely applied to analyse

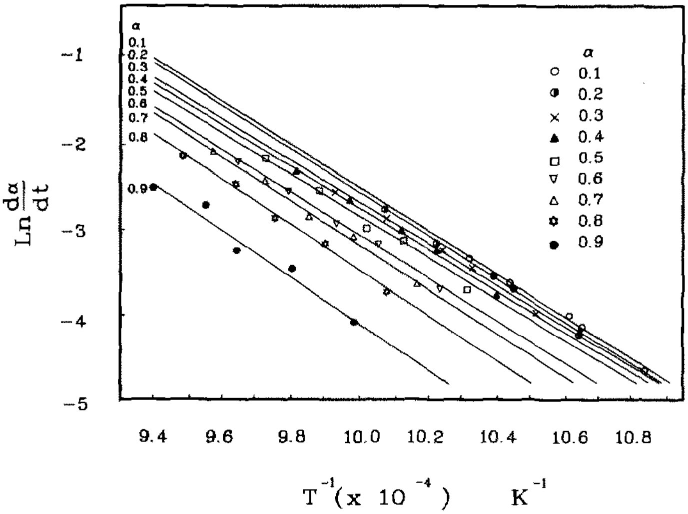

Fig. 7. Plots of $\ln(d\alpha/dt)_i$ vs. $1/T_i$ for each α_i of the thermal decomposition of $CaCO_3$ in an air atmosphere.

TABLE 2

Activation energy and frequency factors according to degree of conversion in the thermal decomposition reaction of $CaCO_3$

α	E	ln A	α	E	ln A
0.1	49.79	22.63	0.6	49.02	22.31
0.2	49.73	22.63	0.7	50.55	23.07
0.3	47.09	21.27	0.8	52.28	23.92
0.4	47.57	21.53	0.9	53.13	24.67
0.5	47.87	21.71			

the mechanism and kinetic parameters of solid state reactions from non-isothermal TG data.

ACKNOWLEDGEMENTS

The authors thank M.S. Woo, Y.K. Kim and Y.W. Kim for their assistance.

REFERENCES

1 H.L. Friedman, J. Polym. Sci. Polym. Chem. Ed., 6 (1964) 183.
2 Y. Masuda, Y. Ito, R. Ito and K. Iwata, Thermochim. Acta, 99 (1986) 205.
3 J.H. Flynn, J. Therm. Anal., 34 (1988) 367.
4 C.D. Doyle, J. Appl. Polym. Sci., 5 (1961) 285.
5 J. Zsako, J. Phys. Chem., 72 (1968) 2406.
6 T. Ozawa, Bull. Chem. Soc. Jpn., 38 (1965) 1881.
7 V. Satava and F. Skvara, J. Am. Ceram. Soc., 52 (1969) 591.
8 L. Reich and S.S. Stivala, Thermochim. Acta, 59 (1982) 247.
9 J.M. Criado, Thermochim. Acta, 24 (1978) 186.
10 J.M. Criado, J. Malek and A. Ortega, Thermochim. Acta, 147 (1989) 377.
11 S. Boy and K. Boehme, Thermochim. Acta, 20 (1977) 195.
12 J. Šesták and G. Berggren, Thermochim. Acta, 3 (1971) 1.